420
GEOME 2
Manuscript received: February 3, 2025
Accepted: April 9, 2025

Geologica Macedonica, Vol. **39**, No. 1, pp. 47–55 (2025)
On print ISSN 0352 – 1206
On line ISSN 1857 – 8586
UDC: 550.348.098.33:624.131.551.042.7
https://doi.org/10.46763/GEOL2539147kv

Original scientific paper

ANALYSIS OF DISCRETIZATION ERRORS IN MICROTREMOR MEASUREMENTS

Mirjana Kocaleva Vitanova, Vlado Gičev

Faculty of Computer Science, Goce Delcev University – Stip,
Krste Misirkov 10A, Štip, Republic of North Macedonia
mirjana.kocaleva@ugd.edu.mk

A b s t r a c t: This study investigates the effects of discretization errors on the analysis of microtremor vibrations measured in a building located in Berovo, using the EQR120 accelerometer. The primary focus is on the impact of discretization on Fourier spectral amplitudes and the accuracy of frequency domain analysis. The results show that with increasing recording time (*T*), there are more pronounced peaks in the Fourier spectrum, especially for higher frequencies. Despite variations in discrete levels of acceleration, the frequency domain response of the instrument remains nearly constant over a wide range of frequencies, resembling white noise. The study highlights that microtremor amplitudes are generally small, and significant variations in spectral amplitudes were not observed over time in a 24 hour measurement period. The findings suggest that external excitation with larger forces is needed to observe spectral peaks, particularly in the ground floor movements. The analysis provides valuable insights into the behavior of microtremors in built environments and emphasizes the challenges of capturing small-scale vibrations in densely populated areas.

Key words: discretization; microtremors; Fourier spectrum; measurement accuracy; building vibrations

INTRODUCTION

Discretization error arises in numerical methods when continuous mathematical models are approximated using discrete representations. This error occurs in various fields such as computational physics, engineering, and numerical simulations, where differential equations are solved using finite difference, finite element, or finite volume methods. The primary sources of discretization error include truncation errors from approximating derivatives and interpolation errors due to the discretization of continuous functions.

Understanding discretization error is essential for ensuring the accuracy and stability of numerical solutions. The error can be analyzed using methods such as error estimation, grid refinement studies, and convergence analysis. A key aspect of discretization error analysis is determining the order of accuracy of a numerical method, which describes how the error decreases as the grid resolution increases.

The discretization error is a significant factor in the measurement and analysis of weak vibrations, such as microtremors. It arises due to the limited resolution of measurement instruments and the digitization processes of continuous signals. In this context, measurements conducted in a house in Berovo (Figure 16a) using the EQR120 instruments indicate that the recording threshold level is 0.0024 cm/s², meaning that all measured vibrations with amplitudes close to this threshold may be affected by discretization error (Gičev et al., 2021; Kokalanov et al., 2022).

The EQR120 accelerometers are highly sensitive and capable of detecting ambient noise (Instruments, C. S., 2019). To ensure accuracy, they were first synchronized using GPS antennas connected via the internet. For proper synchronization, the antennas must be placed outdoors with a strong satellite signal to accurately set the time on instruments. By positioning the accelerometers near the edges of the roof and recording ambient vibrations along the building's length and width, it is possible to determine the structure's torsional periods (Rahmani & Todorovska, 2014; Sawada, 2004).

These accelerometers are typically operated continuously, with each unit synchronized to Coordinated Universal Time (UTC) through its dedicated GPS receiver, achieving a time accuracy of 1 microsecond. The EQR120 is a triaxial accelerometer equipped with a MEMS servo silicon sensor, offering a dynamic range of 128 dB for frequencies between 0.1 and 20 Hz. It supports a recording range of ±4 g, with a recording threshold level of 2.4 × 10^{-6} g (where g = 9.81 m/s², the acceleration due to gravity), equivalent to 2.4 × 10^{-3} gal (cm/s²). The device maintains high precision, with an offset error of less than ±0.02%, a linearity error under ±0.1%, and a gain error below ±0.08%, across an operating temperature range of –10°C to +60°C (Kocaleva, M., & Gičev, V., 2024).

As the data show, the amplitudes of the measured microtremor accelerations are only 3 to 5 times higher than the recording threshold, which can lead to significant errors in the calculated Fourier spectral amplitudes. These errors may affect the accuracy of data analysis and interpretation, highlighting the need for a detailed examination of the effects of discretization.

To investigate this issue, a numerical experiment was conducted to quantify the errors caused by discretization. This experiment focuses on analyzing the spectral components of the signals and exploring ways to minimize the negative impact of discretization errors on the results.

This study explores the nature of discretization errors, their impact on numerical solutions, and strategies for minimizing them. By analyzing these errors, researchers and engineers can improve numerical models, enhance computational efficiency, and ensure reliable results in scientific and engineering applications.

METHODOLOGY AND RESULTS

Our ambient vibrations measurements were conducted in the house on Berovo Lake (Figure 1). We use accelerometer EQR120 having a recording threshold level 2.4 × 10^{-6} g (g = 9.81 m/s^2 = acceleration due to gravity) or 2.4 × 10^{-3} gal = 0.0024 cm/s².

a)

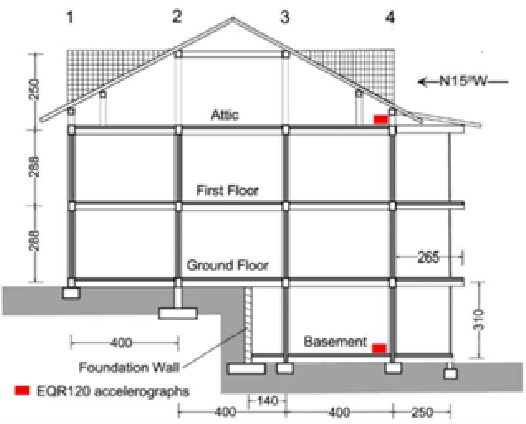

b)

Fig. 1. a) Indoor measurements in a Berovo household b) Positioning of measurement accelerographs

As shown in Figure 2 (top), the amplitudes of the measured microtremor accelerations are only 3 to 5 times higher than this threshold (Kocaleva, M., 2021).

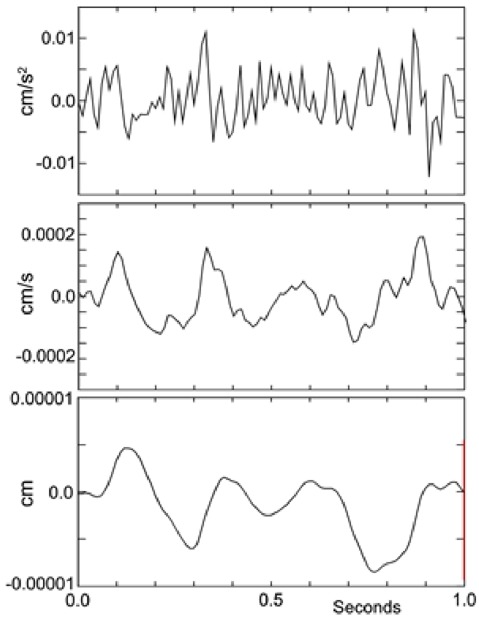

Fig. 2. Spectral amplitudes at the Berovo house

This introduces discretization errors in the calculated Fourier spectral amplitudes, and their effects need to be quantified. To achieve this, the following numerical experiment was conducted.

First, a sine function with an amplitude of a = 0.005 cm/s², a frequency of f = 10 Hz, and a duration of T seconds was generated:

$$g(t) = a \cdot \sin(2 \cdot \pi \cdot f \cdot t) \quad (1)$$

For this function, the Fourier amplitudes were analytically computed. By substituting a and *f*, we obtain: $g(t) = 0.005 \cdot \sin(2 \cdot \pi \cdot 10 \cdot t)$.

The Fourier amplitudes for this function were then calculated using the Fourier transform $G(\omega)$:

$$G(\omega) = \int_0^T g(t)e^{-i\omega t}dt = \int_0^T 0.005 \cdot \sin(2 \cdot 3.14 \cdot 10 \cdot t) \cdot e^{-i\omega t}dt = 0.005 \cdot \int_0^T \sin(62.8t) \cdot e^{-i\omega t}\, dt =$$
$$0.005\left[\left[\frac{62.8 \cdot \cos(\omega t) \cdot \cos(62.8 \cdot t) + \omega \cdot \sin(\omega t) \cdot \sin(62.8 \cdot t)}{\omega^2 - 3943.84}\Big|_0^T\right] - i\left[\frac{62.8 \cdot \cos(62.8 \cdot t) \cdot \sin(\omega t) - \omega \cdot \sin(62.8 \cdot t) \cdot \cos(\omega t)}{\omega^2 - 3943.84}\Big|_0^T\right]\right] \quad (2)$$

As seen in equation (2), the amplitudes $G(\omega)$ depend on the duration of the sine function, i.e., the upper limit of the integral, *T*. For different values of *T*, we will compute and plot the Fourier amplitudes as expressed by equation (2).

a) For *T* = 5 minutes = 300 seconds:

$$G(\omega) = 0.005\left[\left[\frac{62.8 \cdot \cos(300\omega) \cdot (-0.991413) + \omega \cdot \sin(300\omega) \cdot (0.13076799) - 62.8}{\omega^2 - 3943.84}\right] - i\left[\frac{62.8 \cdot (-0.991413) \cdot \sin(300\omega) - \omega \cdot (0.13076799) \cdot \cos(300\omega)}{\omega^2 - 3943.84}\right]\right]$$

b) For *T* = 10 minutes = 600 seconds:

$$G(\omega) = 0.005\left[\left[\frac{62.8 \cdot \cos(600\omega) \cdot (0.96579947) + \omega \cdot \sin(600\omega) \cdot (-0.25929016) - 62.8}{\omega^2 - 3943.84}\right] - i\left[\frac{62.8 \cdot (0.96579947) \cdot \sin(600\omega) - \omega \cdot (-0.25929016) \cdot \cos(600\omega)}{\omega^2 - 3943.84}\right]\right]$$

c) For *T* = 30 minutes = 1800 seconds:

$$G(\omega) = 0.005\left[\left[\frac{62.8 \cdot cos(1800\omega) \cdot (0.70607131) + \omega \cdot sin(1800\omega) \cdot (-0.70814074) - 62.8}{\omega^2 - 3943.84}\right] - i\left[\frac{62.8 \cdot (0.70607131) \cdot sin(1800\omega) - \omega \cdot (-0.70814074) \cdot cos(1800\omega)}{\omega^2 - 3943.84}\right]\right]$$

d) For *T* = 60 minutes = 3600 seconds:

$$G(\omega) = 0.005\left[\left[\frac{62.8 \cdot \cos(3600\omega) \cdot (-0.0029266) + \omega \cdot \sin(3600\omega) \cdot (-0.99999572) - 62.8}{\omega^2 - 3943.84}\right] - i\left[\frac{62.8 \cdot (-0.0029266) \cdot \sin(3600\omega) - \omega \cdot (-0.99999572) \cdot \cos(3600\omega)}{\omega^2 - 3943.84}\right]\right]$$

We also generate the same sine function:

$$g(t) = a \cdot \sin(2 \cdot \pi \cdot f \cdot t) \quad (3)$$

with an amplitude of $a = 0.005$ cm/s², a frequency of $f = 2.5$ Hz, and a duration of *T* seconds. The Fourier amplitudes for this function are analytically computed.

By substituting *a* and *f*, we obtain:

$$g(t) = 0.005 \cdot \sin(2 \cdot \pi \cdot 2.5 \cdot t)$$

The Fourier amplitudes for this function are then calculated using the Fourier transform $G(\omega)$.

$$G(\omega) = \int_0^T g(t)e^{-i\omega t}dt = \int_0^T 0.005 \cdot \sin(2 \cdot 3.14 \cdot 2.5 \cdot t) \cdot e^{-i\omega t}dt = 0.005 \cdot \int_0^T \sin(15.7t) \cdot e^{-i\omega t}\, dt$$
$$= 0.005\left[\left[\frac{15.7 \cdot \cos(\omega t) \cdot \cos(15.7 \cdot t) + \omega \cdot \sin(\omega t) \cdot \sin(15.7 \cdot t)}{\omega^2 - 246.49}\Big|_0^T\right] - i\left[\frac{15.7 \cdot \cos(15.7 \cdot t) \cdot \sin(\omega t) - \omega \cdot \sin(15.7 \cdot t) \cdot \cos(\omega t)}{\omega^2 - 246.49}\Big|_0^T\right]\right]$$

As seen in equation (3), the amplitudes $G(\omega)$ depend on the duration of the sine function, i.e., the upper limit of the integral, T. For different values of T, we will compute and plot the Fourier amplitudes as expressed by equation (3).

a) For T = 5 minutes = 300 seconds:

$$G(\omega) = 0.005\left[\left[\frac{15.7\cdot\cos(600\omega)\cdot(0.0655248097)+\omega\cdot\sin(600\omega)\cdot(0.99785094042)-15.7}{\omega^2-246.49}\right] - i\left[\frac{15.7\cdot(0.0655248097)\cdot\sin(600\omega)-\omega\cdot(0.99785094042)\cdot\cos(600\omega)}{\omega^2-246.49}\right]\right]$$

b) For T = 10 minutes = 600 seconds:

$$G(\omega) = 0.005\left[\left[\frac{15.7\cdot\cos(600\omega)\cdot(0.0655248097)+\omega\cdot\sin(600\omega)\cdot(0.99785094042)-15.7}{\omega^2-246.49}\right] - i\left[\frac{15.7\cdot(0.0655248097)\cdot\sin(600\omega)-\omega\cdot(0.99785094042)\cdot\cos(600\omega)}{\omega^2-246.49}\right]\right]$$

c) For T = 30 minutes = 1800 seconds:

$$G(\omega) = 0.005\left[\left[\frac{15.7\cdot cos(1800\omega)\cdot(-0.19544910584)+\omega\cdot sin(1800\omega)\cdot(-0.98071384563)-15.7}{\omega^2-246.49}\right] - i\left[\frac{15.7\cdot(-0.19544910584)\cdot sin(1800\omega)-\omega\cdot(-0.98071384563)\cdot cos(1800\omega)}{\omega^2-246.49}\right]\right]$$

d) For T = 60 minutes = 3600 seconds:

$$G(\omega) = 0.005\left[\left[\frac{15.7\cdot\cos(3600\omega)\cdot(-0.92359929405)+\omega\cdot\sin(3600\omega)\cdot(0.38335928843)-15.7}{\omega^2-246.49}\right] - i\left[\frac{15.7\cdot(-0.92359929405)\cdot\sin(3600\omega)-\omega\cdot(0.38335928843)\cdot\cos(3600\omega)}{\omega^2-246.49}\right]\right]$$

First, we represent the function for 10 Hz and 2.5 Hz on a time axis (Figure 3). We observe that for 10 Hz, the period is 0.1 second, while for 2.5 Hz, the period is 0.4 seconds.

The frequency domain response $G(\omega)$ is plotted using 1000 points (Figures 4 and 5). The ordinate values $G(\omega)$ are obtained for an angular frequency interval ω ranging from 0 to 100 rad/s with an increment of 0.1 rad/s. We observe that the peak for all sine wave durations T appears at ω = 20π = 62.8 rad/s (Figure 4) and ω = 5π = 15.71 rad/s (Figure. 5), which correspond to f = 10 Hz (Figure 6) and f = 2.5 Hz (Figure 7), respectively.

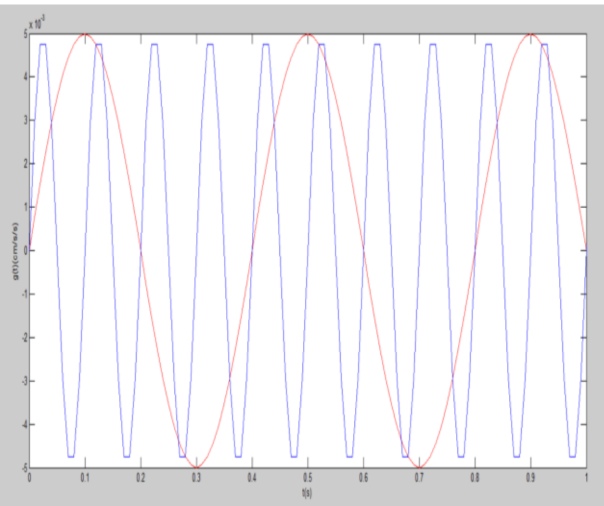

Fig. 3. $g(t)$ for 10 Hz (blue color) and 2.5 Hz (red color)

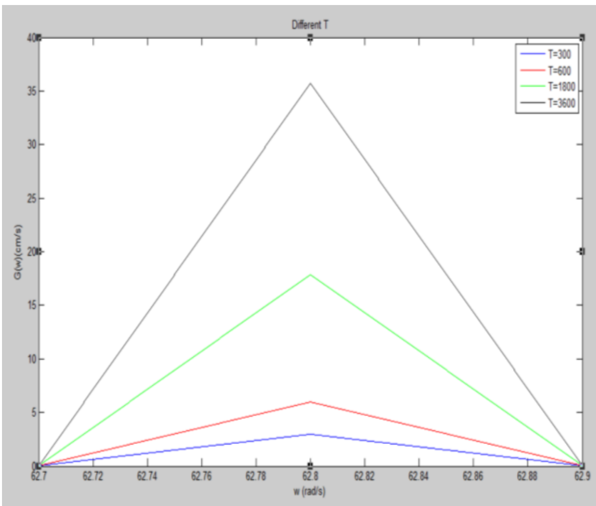

Fig. 4. The peak for all sine wave durations for T = 5, 10, 30 and 60 minutes for f = 10 Hz

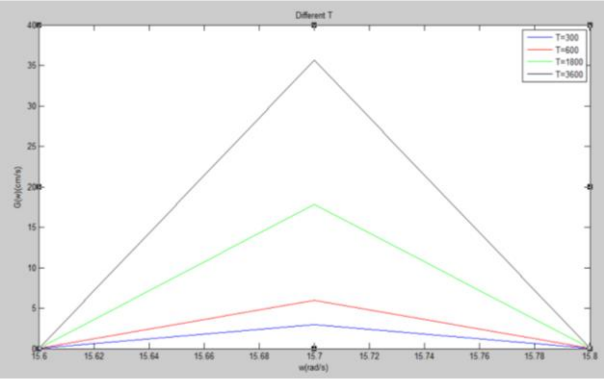

Fig. 5. The peak for all sine wave durations for $T = 5$, 10, 30, and 60 minutes for $f = 2.5$ Hz

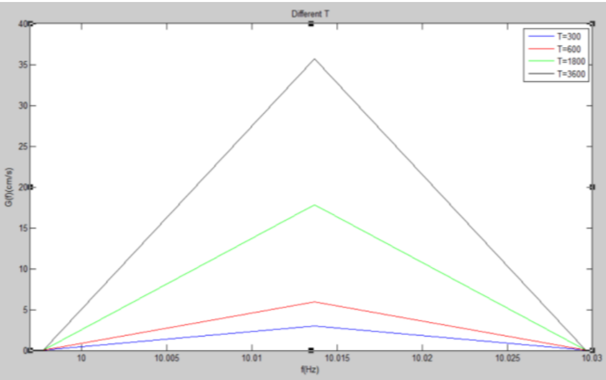

Fig. 6. Fourier spectral amplitudes for $T = 5$, 10, 30, and 60 minutes for $f = 10$ Hz

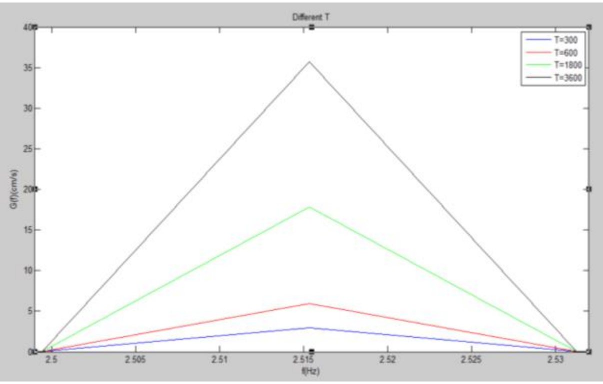

Fig. 7. Fourier spectral amplitudes for $T = 5$, 10, 30, and 60 minutes for $f = 2.5$ Hz

With this, we have verified the analytical solution (1). We observe that for different durations T, the peak at $f = 10$ Hz and $f = 2.5$ Hz varies in magnitude and increases as T increases.

Next, we take the same sine function and digitize it numerically by discretizing the time axis at a sampling frequency of 100 Hz (i.e., 100 points per second or a time interval of $\Delta t = 0.01$ s), while varying the discrete levels on the amplitude axis.

We will work with discrete amplitude levels of 0.0024 cm/s², 0.001 cm/s², 0.0001 cm/s², and 0.00001 cm/s².

For a discrete level of 0.0024 cm/s², the function appears as shown in Figure 8.

Discretization with a discrete level of 0.001 cm/s² results in the following representation of the function (Figure 9).

For a discrete level of 0.0001 cm/s², the function appears as shown in Figure 10.

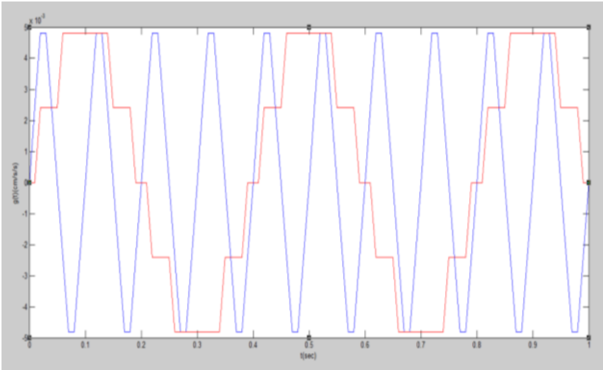

Fig. 8. Function $g(t)$ with discrete level 0.0024 cm/s² (blue 10 Hz, red 2.5 Hz)

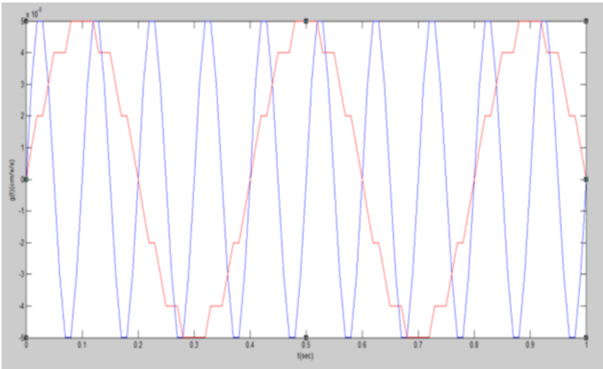

Fig. 9. Function $g(t)$ with discrete level 0.001 cm/s² (blue 10 Hz, red 2.5 Hz)

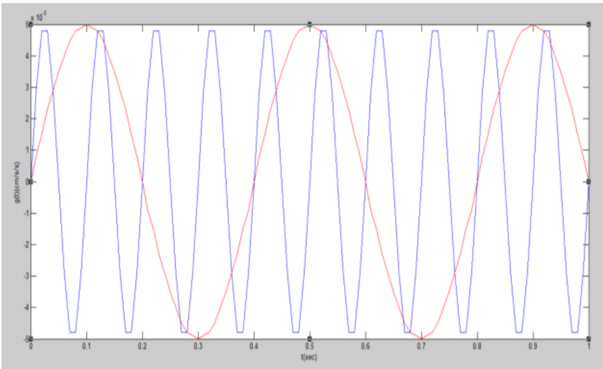

Fig. 10. Function $g(t)$ with discrete level 0.0001 cm/s² (blue 10 Hz, red 2.5 Hz)

Finally, for a discrete level of 0.00001 cm/s², the function appears as shown in Figure 11.

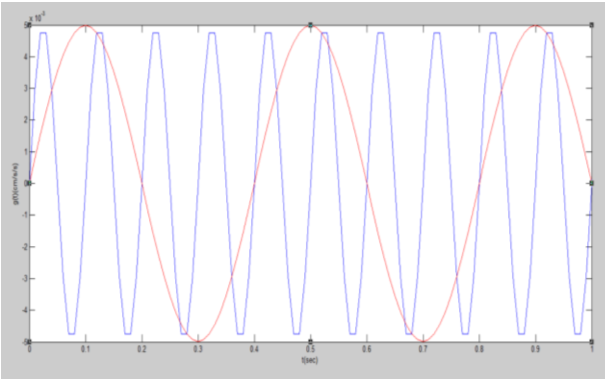

Fig. 11. Function g(t) with discrete level 0.00001 cm / s² (blue 10 Hz, red 2.5 Hz)

From Figures 8 to 11, we observe that no matter how fine the discretization in acceleration is, if the time discretization remains coarse, the accuracy does not improve. This effect is particularly notice-able at higher frequencies (blue lines), where the signal remains imprecise despite finer amplitude discretization. However, for lower frequencies (red lines), this limitation is less significant. For a frequency of 2.5 Hz, we can see that increasing the number of discretization levels results in a smoother signal. Specifically, at the smallest discrete level of 0.00001 cm/s², the graph appears the most accurate– almost identical to Figure 3.

Next, using the FFT routine, we calculate the spectral amplitudes for $T = 5$, 10, 30, and 60 minutes and compare them with the spectra obtained from analytical calculations.

In Figure 12 left and right, a grouped plot of the four discretization levels for $T = 5$ minutes is presented. In Figure 13, a grouped plot of the four discretization levels for $T = 10$ minutes is presented. In Figure 14, a grouped plot of the four discretization levels for $T = 30$ minutes is presented. In Figure 15, a grouped plot of the four discretization levels for $T = 60$ minutes is presented.

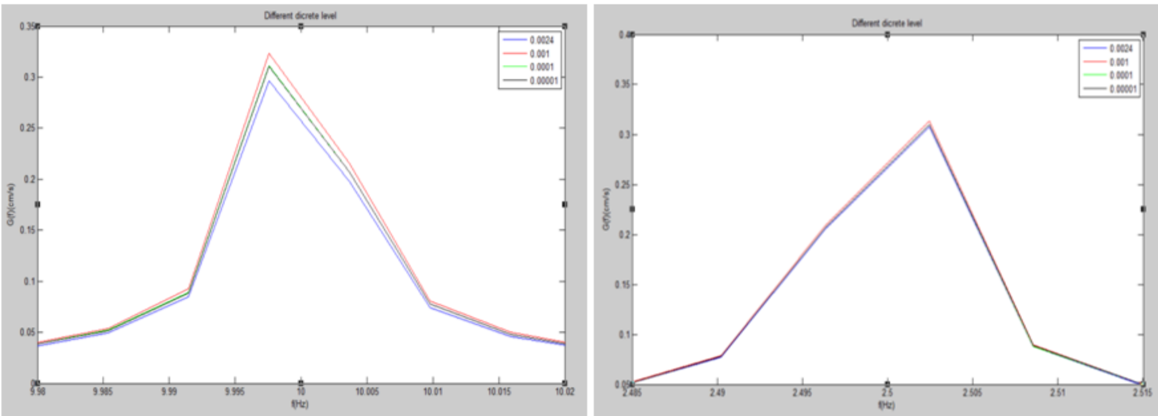

a) b)

Fig. 12. Group graph of the four levels of discretization for $T = 5$ minutes: a) for $f = 10$ Hz (left), b) for $f = 2.5$ Hz (right)

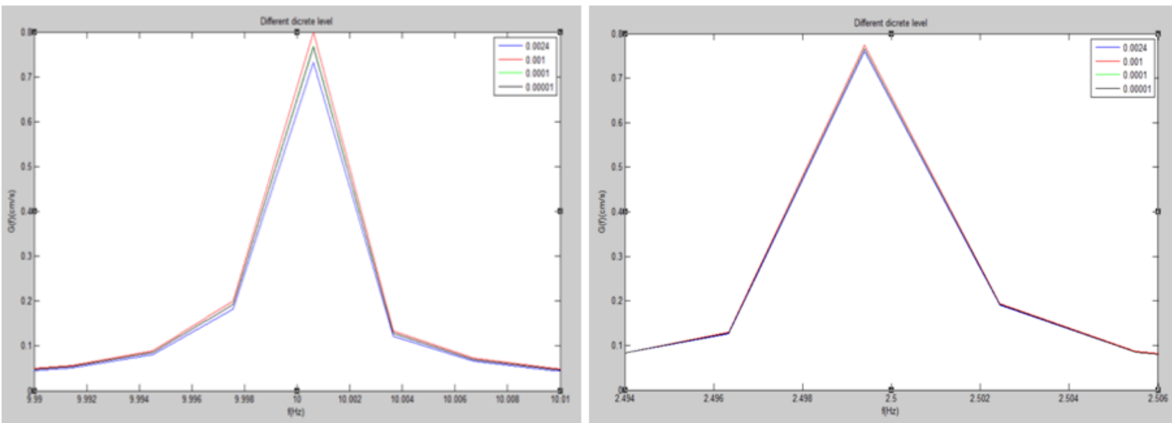

a) b)

Fig. 13. Group graph of the four levels of discretization for $T = 10$ minutes: a) for $f = 10$ Hz (left), b) for $f = 2.5$ Hz (right)

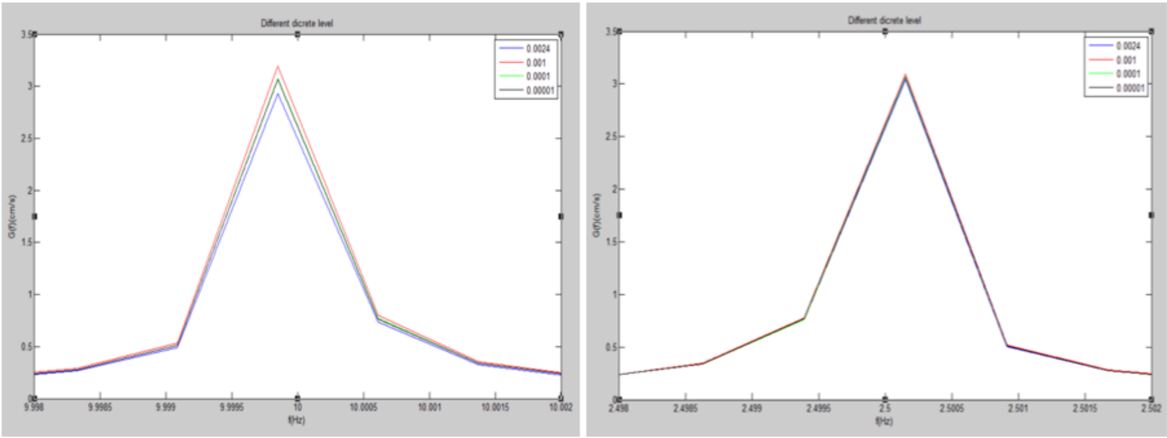

a) b)

Fig. 14. Group graph of the four levels of discretization for $T = 30$ minutes: a) for $f = 10$ Hz (left), b) for $f = 2.5$ Hz (right)

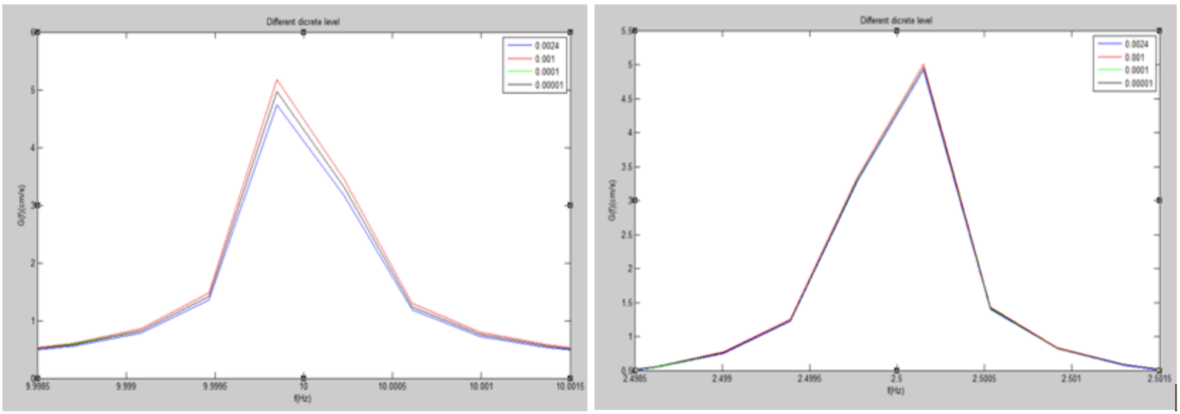

a) b)

Fig. 15. Group graph of the four levels of discretization for $T = 60$ minutes: a) for $f = 10$ Hz (left), b) for $f = 2.5$ Hz (right)

The Table 1 presents a numerical solution to the problem. As observed from the graphs, the ampli-tude of the function varies for different T at frequencies of 10 Hz and 2.5 Hz.

For $T = 300$ seconds, the amplitude is approximately 0.29 – 0.32 cm/s. For $T = 600$ seconds, it ranges from 0.73 to 0.79 cm/s. For $T = 1800$ seconds, it falls within 2.9 – 3.1 cm/s. For $T = 3600$ seconds, it exceeds 4.74 cm/s.

For a frequency of 2.5 Hz, considering the discretization levels, the numerical solution yields similar amplitude values as for 10 Hz:

$T = 300$ seconds → amplitude above 0.3 cm/s

$T = 600$ seconds → amplitude around 0.76 cm/s

$T = 1800$ seconds → amplitude between 3.04 – 3.09 cm/s

$T = 3600$ seconds → amplitude around 4.9 – 5.013 cm/s.

T a b l e 1

Results from numerical solutions

Time (s)	Numerical solution (amplitude) (cm/s) 10 Hz				Numerical solution (amplitude) (cm/s) 2/50 Hz			
	0.0024	0.001	0.0001	0,00001	0.0024	0.001	0.0001	0.00001
300	0.2984	0.3233	0.311	0.31	0.3075	0.3132	0.3095	0.3100
600	0.7327	0.7993	0.7689	0.7679	0.7603	0.7745	0.7654	0,7669
1800	2.931	3.1970	3.075	3.0679	3.0415	3.0983	3.0618	3.0678
3600	4.7423	5.1731	4.9755	4.964	4.9211	5.013	4.9539	4.9636

In this part of the study, by reviewing the previously presented figures and Table 1, we can con-0clude that as the time *T* increases (from 300 to 600, then to 1800, and finally to 3600 seconds), more pronounced nounced peaks appear in the Fourier spectrum.

For *f* = 10 Hz, the amplitude values at a discrete level of 0.001 are the highest, while at 0.0024 are the lowest. For discrete levels of 0.0001 and 0.00001 the amplitudes are approximately equal with values between those of discrete levels 0.0024 and 0.001.

For lower frequency, *f* = 2.5 Hz, the amplitude curves at different discrete levels are closer. All the curves for different values of *T* exhibit the same shape, as shown in Figure 16. Figure 16 provides a graphical representation of the longest 60 minute recording.

Points 1 to 4 represent the four discrete levels.

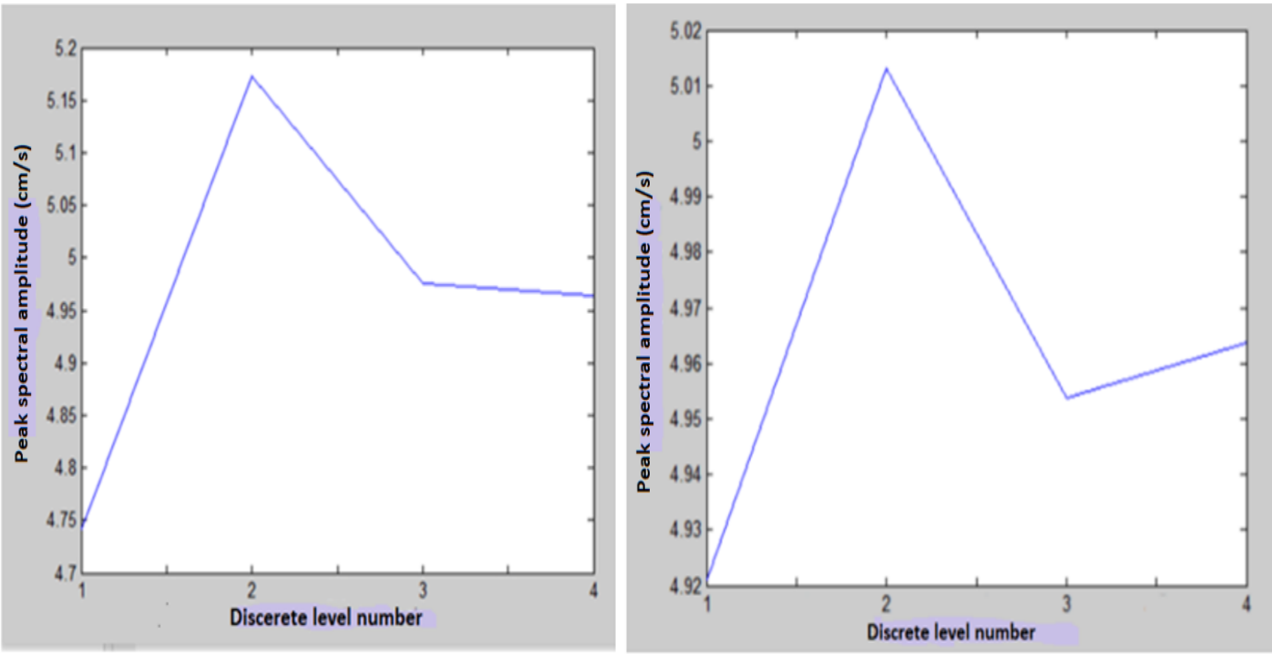

Fig. 16. Numerical solution for peak spectral amplitudes for duration of sine function *T* = 3600 seconds and for four different discrete amplitude levels (1 – 0.0024, 2 – 0.001, 3 – 0.0001, and 4 – 0.00001)
a) *f* = 10 Hz (left), b) *f* = 2.5 Hz (right)

CONCLUSION AND SUMMARY

In densely populated areas, the amplitudes of microtremors tend to be higher in the early afternoon hours and lower during the night. We presented the Fourier amplitude spectra of the recorded microtremors in the basement of a building for various periods throughout a 24 hour period (Figure 1b). We did not find variations in the spectral amplitudes over time. We concluded that, at this location, the contribution to the microtremors, with very small amplitudes, is only a few times greater than the lower threshold of the instrument's recording capability.

Additionally, we observed that in the frequency domain, the response of the instrument is nearly constant over a wide frequency range of interest, from 1 Hz to 20 Hz, resembling white noise. Because of the low excitation in this quiet environment, with our FFT routine we did not find peaks in the transfer functions for the measurements in the basement and the ground floor.

The ground floor movements at the building's characteristic frequencies are not zero, but they are small compared to the amplitudes of ground noise. It will be necessary to excite the building with significant external forces for spectral peaks to appear in the ground floor motion. Movements in the basement and garage are slightly smoothed microtremor motions in the underlying bedrock near the building. This smoothing occurs due to the large surfaces covered with reinforced concrete.

REFERENCES

Gičev, V.; Trifunac, M. D.; Todorovska, M. I.; Kocaleva, M.; Stojanova, A. & Kokalanov, V. (2021): Ambient vibration measurements in an irregular building. *Soil Dynamics and Earthquake Engineering*, Volume **141**, pp. 1–22. ISSN 0267-7261. https://doi.org/10.1016/j.soildyn.2020.106484

Instruments, C. S. (2019): EQResponder: New generation plug-and-play accelerometer from CSI Technical Manual.

Kocaleva, M. (2021). *Natural periods of civil engineering objects obtained by measuring and processing of ambient vibrations tests*. PhD thesis, Faculty of Computer Science, Goce Delčev University, Štip.

Kocaleva, M. and Gičev, V. (2024): Analysis of microtremors by measuring and processing of ambient vibrations tests. *Geologica Macedonica*, **38** (2). pp. 105–114.

Kokalanov, V., Trifunac, M., Gičev, V., Kocaleva, M., Stojanova, A. (2022): High frequency calibration of a finite element model of an irregular building via ambient vibration measurements. *Soil Dynamics and Earthquake Engineering*, Volume **153**. 107005. ISSN 0267–7261. https://doi.org/10.1016/j.soildyn.2021.107005

Rahmani, M., Todorovska, M. I. (2014): 1D System identification of a 54-story steel frame building by seismic interferometry. *Earthquake Engineering and Structural Dynamics*. 43, 627–640. https://doi.org/10.1002/eqe.2364

Sawada, S. (2004): A simplified equation to approximate natural period of layered ground on the elastic bedrock. *13th World Conference on Earthquake Engineering*, 1100.

Р е з и м е

АНАЛИЗА НА ДИСКРЕТИЗАЦИСКИТЕ ГРЕШКИ ВО МЕРЕЊАТА НА МИКРОТРЕМОРИ

Мирјана Коцалева Витанова, Владо Гичев

Факултет за информатика, Универзитет „Гоце Делчев“
Крсте Мисирков 10А, Штип, Република Северна Македонија
mirjana.kocaleva@ugd.edu.mk.

Клучни **зборови:** дискретизација; микротремори; Фуриев спектар; точност на мерење; вибрации на згради

Оваа студија ги истражува влијанијата на дискретизациските грешки при анализата на вибрации на микротремори измерени во зграда лоцирана во Берово, користејќи го акцелерометарот EQR120. Главниот фокус е на влијанието на дискретизацијата на Фуриевите спектрални амплитуди и точноста на анализа во фреквенцискиот домен. Резултатите покажуваат дека со зголемување на времето на снимање (*T*), се појавуваат поизразени пикови во Фуриевиот спектар, особено за повисоки фреквенции. Без разлика на варијациите во дискретните нивоа на забрзување, одговорот на инструментот во фреквенцискииот домен останува речиси константен во широк опсег на фреквенции, што наликува на бел шум. Студијата истакнува дека амплитудите на микротреморите генерално се мали, и значителни варијации во спектралните амплитуди не се забележани во текот на 24-часовниот период на мерење. Наодите сугерираат дека е потребно надворешно возбудување со поголеми сили за да се забележат спектрални пикови, особено при движењата на приземјето. Анализата дава вредни сознанија за однесувањето на микротреморите во изградените објекти и ги нагласува предизвиците за препознавање на вибрации од мал обем во густо населените области.